Published in final edited form as:
Clin Cancer Res. 2009 May 1; 15(9): 3126–3134. doi:10.1158/1078-0432.CCR-08-2666.

A Potent, Imaging Adenoviral Vector Driven by the Cancer-selective Mucin-1 Promoter That Targets Breast Cancer Metastasis

Steven T. Huyn[1], **Jeremy B. Burton**[1], **Makoto Sato**[1], **Michael Carey**[2], **Sanjiv S. Gambhir**[5], and **Lily Wu**[1,3,4]

[1]Department of Molecular and Medical Pharmacology, David Geffen School of Medicine, University of California at Los Angeles (UCLA) School of Medicine, Los Angeles, California

[2]Department of Biological Chemistry, David Geffen School of Medicine, University of California at Los Angeles (UCLA) School of Medicine, Los Angeles, California

[3]Department of Urology, David Geffen School of Medicine, University of California at Los Angeles (UCLA) School of Medicine, Los Angeles, California

[4]Institute of Molecular Medicine, and Jonsson Comprehensive Cancer Center, David Geffen School of Medicine, University of California at Los Angeles (UCLA) School of Medicine, Los Angeles, California

[5]BIO-X, Stanford University School of Medicine, Stanford, California

Abstract

Purpose—With breast cancer, early detection and proper staging are critical, and will often influence both the treatment regimen and the therapeutic outcome for those affected with this disease. Improvements in these areas will play a profound role in reducing mortality from breast cancer.

Experimental Design—In this work we developed a breast cancer – targeted serotype 5 adenoviral vector, utilizing the tumor-specific mucin-1 promoter in combination with the two-step transcriptional amplification system, a system used to augment the activity of weak tissue – specific promoters.

Results—We showed the strong specificity of this tumor-selective adenovirus to express the luciferase optical imaging gene, leading to diagnostic signals that enabled detection of sentinel lymph node metastasis of breast cancer. Furthermore, we were able to target hepatic metastases following systemic administration of this mucin-1 selective virus.

Conclusions—Collectively, we showed that the amplified mucin-1 promoter – driven vector is able to deliver to and selectively express a desirable transgene in metastatic lesions of breast tumors. This work has strong clinical relevance to current diagnostic staging approaches, and could add to targeted therapeutic strategies to advance the fight against breast cancer.

Breast cancer is the second leading cause of cancer-related death in women in the United States, accounting for an estimated 26% of all new cancer cases (1). In 2008 alone it was estimated that approximately 180,000 women were diagnosed with breast cancer, while over 40,000 died because of this disease.[6] As is the case with most cancers, metastasis is the primary cause of

Requests for reprints: Lily Wu, Department of Urology, MRL 2210, Box 951738, University of California, Los Angeles, CA 90095-1738. Phone: 310-825-8511; Fax: 310-206-3027; LWu@mednet.ucla.edu.

Disclosure of Potential Conflicts of Interest: No potential conflicts of interest were disclosed.

mortality associated with breast cancer. Data assessing the 5-year relative survival rates of women diagnosed with breast cancers indicate a 6-fold increase in survival in women diagnosed with early-stage breast cancers, compared with those with advanced-stage breast tumors (2). Although detection and staging modalities of breast cancers have advanced significantly over the last decade, further effort is needed to ensure that mortality associated with this disease is decreased.

The spread of cancer cells to regional lymph nodes occurs through the lymphatic vasculature and is the first step in the dissemination of breast cancers (3). Hence, lymph node metastasis is a significant prognostic indicator in the course of this disease and often dictates therapeutic aggressiveness. A commonly used method to assess nodal status is the sentinel lymph node biopsy, which is based on the removal and histopathologic examination of the first draining, or sentinel lymph node, as determined by lymphatic uptake of radiolabeled colloids or dyes. In sentinel lymph node biopsy, the administration of lymphotropic dyes or radiolabeled colloids will drain through tumor-associated lymphatic vessels, leading to the localization of sentinel lymph nodes by visual inspection or through the use of a γ camera in the case of dyes or 99-technetium labeled colloids, respectively (4). However, sentinel lymph node biopsy is invasive and can lead to complications, such as shoulder dysfunction, nerve damage, upper arm numbness, and lymphedema (5). Thus, there is a great need for highly sensitive, accurate, and yet noninvasive detection modalities. Of interest, recent reports by our group and others illustrated through careful *in vivo* biodistribution studies that human serotype 5 adenoviral vectors (Ad) can traffic effectively into regional lymph nodes (6). In much the same way as the other lymphotropic agents, the uptake of adenovirus is influenced by its size (~ 100 nm) and charge (6,7). Moreover, its lymphotrophic properties can be exploited to detect nodal metastases by incorporating imaging reporter genes into the adenoviral vector (7,8).

Systemic targeting of metastatic tumors cells is the ultimate goal in the field of cancer gene therapy and can potentially play an important role in reducing mortality from this disease. Several features of the recombinant adenovirus make it an attractive vehicle for the delivery of therapeutic genes to metastatic lesions. They include its ability to transduce a wide array of tissues and the established technology to incorporate exogenous genetic elements into the viral genome. However, in order for this type of therapy to have clinical impact, the obstacles of specificity and efficiency need to be overcome. We have worked to address these issues by using the two-step transcriptional amplification (TSTA) method (Fig. 1A), a system developed to boost the activity of a tumor-specific promoter, through the potent transcriptional activator, VP16 (9–11). To ensure tumor-restricted expression, the mucin-1 (MUC1) promoter (-780 to +50) was utilized (12–14). Mucins are large transmembrane proteins, thought to be involved in cell signaling and cell-cell adhesion (15). In many cancers, the aberrant overexpression of this surface protein is thought to contribute to both metastasis and immune evasion (15–17). Furthermore, MUC1 has been determined to be one of the most frequently expressed surface markers in metastatic breast cancers. One study evaluating tumors from 44,000 terminal cases determined that approximately 80% expressed MUC1 (18). Based on these observations, the MUC1 protein has garnered interest as a target for immunotherapy of adenocarcinomas and several MUC1-based cancer vaccines have been developed (19). Furthermore, multiple groups have successfully applied this promoter in transcriptional targeting strategies of various cancers, including breast cancer (12,20).

Translational Relevance

This study illustrates the proof-of-principle of a novel technology to detect metastatic breast cancers. By engineering a recombinant adenoviral vector to produce imaging signal

[6]Cancer Stat Facts Sheet, http://seer.cancer.gov/statfacts/html/breast.html.

exclusively in a cancer-selective manner, our aim is to create a vehicle that can seek out and achieve functional molecular imaging of metastatic lesions in living subjects. In this study we combined optical imaging with clinically relevant positron emission tomography to specifically identify lymph node and liver metastases. Compared with conventional staging methods that require surgical biopsy of draining lymph nodes, the noninvasive and specific nature of our functional imaging enables the direct mapping of nodal involvement, and hence the prospect of reduced complications of this procedure. Another promising advantage of our gene expression – based strategy is that we can easily integrate the simultaneous expression of cytotoxic genes with the imaging gene into a single adenoviral vector. In doing so, we can achieve image-guided therapy to treat metastatic disease for breast cancer, as well as other types of cancer.

Here, we developed tumor-targeted adenoviral vectors that express the firefly luciferase imaging reporter gene, under the MUC1 promoter – driven TSTA system. This AdMUC1-TSTA-fl vector exhibited high specificity and augmented activity for breast tumor cells. In animal experimentations, as proof of principle, we showed the ability of AdMUC1-TSTA-fl to detect lymph node metastasis as well as experimental hepatic metastasis of breast cancer. We believe that this system holds promise to be a useful tool for the clinical management of advanced-stage breast cancer.

Materials and Methods

Adenoviral generation

Adenoviral vectors were constructed based on the AdEasy system (21). Virus was propagated, purified, and titered as previously described (9). The tail-to-tail configuration of the AdMUC1-TSTA-fl was constructed by replacing the PSEBC promoter from pShuttleBC-VP2 with a multiple cloning site. The MUC-1 promoter, kindly provided by Dr Noriyuki Kasahara, was subcloned into *Spe*I and *Eco*RV sites in the multiple cloning site, resulting in pShuttleMUC1-VP2. G5-fluc, obtained from pG5-fluc (22), was then inserted into pShuttleMUC1-VP2 in order to generate pShuttleMUC1-TSTA-fl.

Cell lines and cell culture experiments

The HepG2 liver tumor cell line (a kind gift from Dr. Edward McCabe), and the breast cancer cell lines KPL-1 (a kind gift from Dr. Dennis Slamon), MDA-MB-231, MDA-MB-435 (a kind gift from Dr. Luisa Iruela-Arispe), MCF-7, and BT-20 (obtained from the American Type Culture Collection) were all maintained in DMEM containing 10% fetal bovine serum and 1% penicillin/streptomycin. T47D breast cancer cells (obtained from the American Type Culture Collection) were cultured in RPMI containing 10% fetal bovine serum and 1% penicillin/streptomycin.

For transfection experiments, 0.5×10^5 cells were plated in 24-well plates and cotransfected in triplicate with equimolar amounts of either pGL3MUC1 or pMUC1-TSTA-fl and a CMV-β-galactosidase (β-gal) plasmid by standard LipofectAMINE 2000 protocol (Invitrogen). For adenovirus infection experiments, cells were plated at 0.5×10^5 in 24-well plates 24 h prior to infection, and infected with either AdCMV-fl or AdMUC1-TSTA-fl at a multiplicity of inflection of 5 (MOI = 5). Forty-eight hours after transfection or transduction, cells were lysed and assayed by standard luciferase assay (Promega). β-Gal expression assessed by β-gal detection kit II (Clontech) was used to normalize for transfection efficiency.

Tumor xenograft experiments

Marked tumor models were generated by transduction of tumor cells with lentivirus carrying the cytomegalovirus (CMV) promoter-driven renilla luciferase (RL) reporter genes, as previously described (23). To promote lymphatic metastasis, tumor cells were transduced at a multiplicity of infection of 1 (MOI = 1, 1 infectious virus per cell) with a second lentiviral vector, pCCL-CMV-VEGF-C-IRES-EGFP (VEGF-C) or empty vector pCCL-CMV-IRES-EGFP to serve as control (Ctrl). KPL-1/RL tumor cells (5×10^5) were implanted with matrigel into the second mammary fat pad of female SCID/Beige mice. Tumor kinetics were monitored over 4 wk by bioluminescent imaging of renilla luciferase.

In vivo off-target expression analysis

Female Scid/Beige mice were i.v. injected with either AdCMV-fl or AdMUC1-TSTA-fl (1×10^8 pfu/100 μL). The animals were optically imaged for firefly luciferase activity at 5, 10, and 20 d postinjection. Briefly, mice were injected with D-luciferin (150 mg/kg i.p.) and imaged with the bioluminescent imager (IVIS 100; Caliper Life Science Inc.) after a 20-min incubation. At 20 d postinjection the animals were sacrificed and the indicated organs were extracted and imaged *ex vivo*. Data were analyzed using IGOR-PRO Living Image software as described previously (23).

Targeting lymph node metastasis

Mice received peritumoral injections of AdMUC1-TSTA-fl (1×10^8 pfu) 4 wk after mammary pad implantation of KPL-1/VEGF-C cells. Three days after adenovirus injection, the axillary lymph nodes of treated animals were imaged for renilla and firefly luciferase expression, as described previously (8). Briefly, ipsilateral and contralateral lymph nodes were dissected and imaged by successive exposure to D-luciferin and coelentrazine. To minimize signal carryover in this dual imaging technique, the animals first received i.p. injections of D-luciferin. Twenty minutes after substrate administration, the animals were sacrificed, and the lymph nodes were extracted and imaged for firefly luciferase activity *ex vivo*. Lymph nodes were then washed and immersed in PBS for 20 min in order to allow residual firefly signal to bleed off. Lymph nodes were then rinsed in coelantrazine, washed again in PBS, and imaged for renilla luciferase signal. Lymph nodes were then snap-frozen and stored at -80°C. To further correlate firefly and renilla expression levels, lymph nodes were later mechanically homogenized, digested in passive lysis buffer for 20 min, and analyzed for renilla and firefly luciferase expression using the dual luciferase assay kit (Promega).

Targeting hepatic implants

Tumors were allowed to grow over a period of 1 mo, after which time the animals received i.v. injections of AdMUC1-TSTA-fl at 1×10^8 pfu/mouse. The animals were optically imaged for firefly luciferase once a week for a period of 3 wk. Following imaging, the animals were sacrificed and their livers were extracted. Half of each of the four lobes of the liver were fixed in 3% paraformaldehyde, embedded in paraffin, sectioned, and stained with H&E, as described previously (23). The remaining liver lobes were mechanically homogenized, and 10 mg of homogenate were lysed in passive lysis buffer. Five microliters of supernatant were assayed using dual luciferase assay (Promega).

PET/CT imaging

The mice were imaged by positron emission tomography (PET) using 200 μCi of 2-[^{18}F]-fluoro-2-deoxy-D-glucose (^{18}FDG) in a single i.v. bolus and imaged in a Focus 220 micro-PET scanner and MicroCAT II scanner (Siemens Preclinical Solutions) as previously described (8). PET images were created by filtered back projection at 0.4-mm pixel size with 0.8-mm

slice thickness and fused PET-computed tomography (CT) images as previously indicated (24).

Statistical analysis

Characterization of MUC-1 constructs in cell culture experiments was carried out in triplicate, and data are presented as means ± SE. For analysis of VEGF-C – induced lymph node metastasis, data are presented as means ± SE and compared by Student's *t* test. The correlation plot assessing targeting of lymph node metastasis was also analyzed using Student's *t* test.

Results

The development and evaluation of the mucin1 TSTA system

In order to assess the efficiency and specificity of the Mucin1 promoter within the TSTA system, the activity of our pMUC1-TSTA-fl plasmid construct was first compared with a conventional one-step MUC1 direct expression vector (pGL3MUC1) *in vitro* (Fig. 1B). Both pMUC1-TSTA-fl and pGL3MUC1 constructs were transfected into both breast (MCF-7, BT-20, MDA-MB-231) and nonbreast cancer cell lines (HepG2), and firefly reporter activity was assessed. The selected cell lines were chosen based on the variability of their MUC1 expression as assessed in previously published results (15), and confirmed through reverse transcription-PCR analysis (data not shown). In MCF-7 cells, normalized firefly luciferase expression in one-step direct expression construct was observed to be 1,200 ± 90 RLU/s, and was amplified to $2.23 \pm 0.22 \times 10^5$ RLU/s in the MUC1 TSTA construct. In BT-20 cells, normalized one-step firefly luciferase expression was observed to be 850 ± 100 RLU/s, and $2.18 \pm 0.15 \times 10^5$ RLU/s in MUC-1 TSTA transfected cells. Based on these results, we determined that through the use of TSTA, we could amplify MUC-1 promoter expression approximately 180- and 260-fold in MCF-7 and BT-20 breast cancer cells, respectively. The expression profiles between pMUC1-TSTA-fl and pGL3MUC1 in all breast and nonbreast cancer cell lines were nearly identical, indicating that amplification occurs without a loss of promoter specificity. In addition, reporter activity directly correlated with previously established MUC1 expression levels in each cell line, giving further evidence of specificity.

We next integrated the Mucin-1 TSTA construct into an adenoviral vector, generating AdMUC1-TSTA-fl. We then compared the expression levels of this virus with those obtained by a CMV-driven firefly luciferase – expressing adenovirus (AdCMV-fl) in breast cancer (BT20, MCF-7, KPL-1, T47D, MDA-MB231, and MDA-MB435) and nonbreast (HepG2) cell lines, by transducing at a multiplicity of infection of 5 (MOI = 5, 5 infectious virus per cell). AdMUC1-TSTA-fl consistently achieved higher reporter activities than AdCMV-fl in all breast cancer cell lines evaluated (Fig. 1C). The greatest difference in activity was observed in MCF-7 cells, in which firefly luciferase activity was observed to be $1.08 \pm 0.07 \times 10^7$ RLU/s in AdTSTA-MUC1-fl – infected cells compared with $6.72 \pm 1.04 \times 10^5$ RLU/s in the AdCMV-fl – infected cells. In KPL-1 cells, the respective AdTSTA-MUC1-fl and AdCMV-fl activity was $1.25 \pm 0.02 \times 10^7$ and $4.74 \pm 0.85 \times 10^6$ RLU/s.

The off-target expression of AdMUC1-TSTA-fl

It has been well established that applications of adenoviral vectors exhibit a strong tropism for the liver *in vivo* (6). To evaluate the off-target expression of AdMUC1-TSTA-fl in the liver, we compared its activity with that of the strong constitutive AdCMV-fl (Fig. 2). Following i.v. injection with 1×10^7 pfu of each virus, the animals were monitored longitudinally for firefly luciferase expression by bioluminescence imaging. High liver transduction and expression was observed with the AdCMV-fl – injected group ($n = 6$; Fig. 2A). However, due to the tissue selectivity of the MUC-1 promoter, the AdMUC1-TSTA-fl – injected animals ($n = 6$) exhibited no detectable signal in liver despite the majority of virus trafficking to and transducing this

organ (Fig. 2A). The magnitudes of luciferase expression in the major organs of the animals in each treatment group were determined at the day 20 end point by *ex vivo* bioluminescent imaging (Fig. 2B).

KPL-1 xenograft model of breast cancer

We next set out to evaluate the specificity of AdMUC1-TSTA-fl in xenograft models of breast cancer. KPL-1 was recently established as a novel human breast cancer cell line derived from the malignant effusion of a 51-year-old Japanese breast cancer patient (25). Previously published reports (15) and our experience has shown that these cells express high levels of mucin 1 RNA (data not shown). In addition, this model has been shown to exhibit a high tumor take rate *in vivo*. As a result, we elected to use KPL-1 breast tumors for implantation into the mammary fat pads of female SCID-beige mice, in order to evaluate the targeting ability of AdMUC1-TSTA-fl. Robust firefly luciferase signal was detected in the primary tumor after intratumoral injection of 1×10^8 pfu of AdMUC1-TSTA-fl (Fig. 3A). Although a large percentage of the virus accumulates in the primary tumor, our prior experience indicates that systemic leakage of viral vector is common after tumor-directed injection leading to signal in distant sites such as the liver (11,26). This is due in large part to the high affinity of the virus for this organ. The lack of systemic signal outside of the tumor (Fig. 3A) again reaffirms the tumor-selective expression of AdMUC1-TSTA-fl.

Inducing lymph node metastasis in KPL-1 tumors by VEGF-C overexpression

Based on our experience, the orthotopic KPL-1 xenografts, established in mammary fat pads of immune deficient mice, displayed a low incidence of nodal metastasis following implantation of 5×10^5 cells. To augment the rate of nodal metastasis, we induced VEGF-C overexpression in the KPL-1 tumors. Extensive literature supports that enhanced tumoral lymphangiogenesis promotes tumor cell dissemination via lymphatic vasculature to draining lymph nodes (3,27). The dominant lymphatic growth factors are VEGF-C and VEGF-D, which induce lymphatic endothelial cell proliferation and migration through the activation of the receptor, VEGFR-3 (3). Experimental models of breast cancer have shown that VEGF-C expression enhances lymphangiogenesis and subsequent lymph node metastasis (27). In this study, we achieved stable expression of VEGF-C in KPL-1 cells through the use of a lentiviral vector expressing VEGF-C and green fluorescent protein, driven by the CMV promoter (ref. 23; Fig. 3C). The control KPL-1 tumor, lacking VEFG-C overexpression (non VEGF-C, Fig. 3B), was transduced with the lentiviral vector that only expresses green fluorescent protein. To facilitate the tracking of tumor growth and metastasis, all cells were marked with a second lentiviral vector expressing renilla luciferase. Following tumor implantation, animals ($n = 16$) were imaged for renilla luciferase over the course of four weeks (Fig. 3B and C). At the terminal time point, the animals were sacrificed and axillary lymph nodes were extracted and assessed for nodal involvement by renilla luciferase optical signal. Imaging revealed that 0 of 8 non-VEGF-C control tumor-bearing mice exhibited lymph node metastasis (Fig. 3D), whereas 4 of 8 mice bearing VEGF-C–overexpressing KPL-1 tumors had detectable lymph node metastasis ($P < 0.05$; Fig. 3E). A region of interest was taken for each axillary node and the average of optical signal within the region of interest for positive lymph nodes was then compared with the average of all negative nodes (Fig. 3F).

Targeting lymph node metastasis

Next, we tested the ability of the AdMUC1-TSTA-fl to target and detect lymph node metastasis in the above described renilla luciferase – marked KPL-1-VEGF-C orthotopic breast tumors. Targeting experiments were carried out using peritumoral injections of 1×10^8 pfu of AdMUC-1-TSTA-fl after the tumors were grown for approximately four weeks in female SCID beige mice ($n = 8$; Fig. 4A). Three days post-AdMUC-1-TSTA-fl injection, the animals were

sacrificed and both the ipsilateral and contralateral axillary lymph nodes relative to the primary tumor were extracted and assessed for renilla and firefly luciferase expression by sequential *ex vivo* optical imaging (Fig. 4B). Strong optical signals were observed in the ipsilateral lymph nodes of 50% of the treated cohort, including the representative animal (Fig. 4B), showing correlation between the vector-directed firefly luciferase signal and the renilla luciferase tumor signal. To obtain a more precise measurement of these results, we opted to carry out an *in vitro* analysis of both firefly and renilla luciferase expression in the extracted lymph nodes using a dual luciferase assay. Through this analysis we were able to further correlate the presence of lymph node metastasis (renilla luciferase expression) with viral reporter gene expression (firefly luciferase expression). Renilla expression was plotted against firefly luciferase expression giving an R^2 value of 0.689 ($P < 0.05$; Fig. 4C). These findings support that the AdMUC1-TSTA-fl we have created is able to target established MUC1-positive KPL-1 nodal metastasis.

Targeting experimental hepatic metastases

To further scrutinize the tumor selectivity of the MUC-1 – targeted vector, we chose to target liver metastasis by systemic vector administration. This is a clinically relevant scenario, as breast cancer patients with advanced disease will often present with secondary tumors in the liver, lung, and bone (28). For this set of experiments, 5×10^5 KPL-1 cells were surgically implanted into the livers (left lobe) of four-week-old SCID-beige mice ($n = 5$) and 1×10^8 pfu of AdMUC1-TSTA-fl was injected i.v. three weeks after tumor cell implantation. Repetitive imaging for firefly luciferase activity revealed localized signals over the hepatic area, which persisted over the three-week duration of monitoring (Fig. 5A). To achieve more precise three-dimensional localization of the hepatic tumor in the animal, a combined PET-CT modality with ^{18}FDG as the tracer was used. PET imaging revealed a predominant FDG-avid signal in the hepatic region (Fig. 5A). The vector-directed luciferase signal also initiated more prominently in the hepatic region. However, the known tissue-scattering effects of optical signals make their precise localization difficult. However, side by side comparison of virus-injected, non–tumor-bearing control animals suggests that we are able to achieve tumor-specific reporter expression. Interestingly, in the immune deficient setting, the vector-directed luciferase expression was able to persist and increase incrementally over time. Histologic examination of the liver tumor at the end point of the study (35 days after implantation) revealed large well-demarcated tumors (measuring ~ 1 cm) that had invaded extensively into the left lobe of the liver (Fig. 5B). Comparison of optical signal between animals bearing KPL-1 hepatic implanted tumors and control non – tumor-bearing mice ($n = 3$; Fig. 5A), both injected i.v. with the same titer of AdMUC1-TSTA-fl, supports our belief that viral gene expression comes as the result of tumor targeting. Importantly, despite the high amount of virus that is sequestered into liver cells as a result of the viral liver tropism, the strong specificity and robust gene expression of our virus allowed for targeted imaging of these KPL-1 lesions alone. To verify the ability of AdMUC1-TSTA-fl to target the hepatic KPL tumors, the harvested liver of a representative animal (Fig. 5C) was divided by lobe, and assessed for both firefly and renilla luciferase expression. The dual luciferase activity measurements from the distinct lobes again confirmed the correlation between tumor presence and viral gene expression. These results showed the ability of AdMUC1-TSTA-fl to specifically target breast tumors in the liver via i.v. injection.

Discussion

The development of novel targeted tools for use in the early detection and treatment of metastatic breast cancer is critical for reducing mortality associated with this disease. In this current study, a transcriptionally targeted, recombinant adenovirus served as a diagnostic tool by delivering imaging reporter genes to tumor cells, enabling the direct detection and

visualization of tumor metastasis in lymph nodes and liver. This system made use of the tumor-specific MUC1 promoter in conjunction with the TSTA system, a two-tiered amplification scheme that has been applied successfully to modify the prostate-specific antigen promoter (10,22), the VEGF promoter (29), pancreatic-specific cholecystokinin type A receptor promoter (30), and the survivin promoter (31). Through adaptation of TSTA, mucin-1 promoter activity was amplified up to 260-fold, greatly enhancing its sensitivity and efficiency.

Systemic application of Ad vectors has been limited by their strong tropism for the liver, which diminishes gene delivery to other organs (6). Over the years much work has focused on abolishing liver transduction of adenovirus through various strategies. Some include modifications to the adenoviral structure (32,33), retargeting the virus through use of adapters (34), and most recently through ablation of FX-facilitated transduction (35,36). However, strategies to detarget the adenovirus away from the liver have not shown enhanced transduction to extrahepatic target sites. We and others have shown that transcriptionally targeted adenoviral vectors could be a means to safeguard against unwanted liver transduction (11,37). Although a transcriptional targeting strategy will not prevent adenoviral liver infection, it can eliminate viral gene expression in the liver. In this study, we showed that the mucin-1 promoter – driven AdMUC1-TSTA-fl remained transcriptionally silent in the liver due to weak mucin-1 expression in normal liver tissue. Conversely, this cancer-selective imaging Ad can successfully target and produce optical signals to detect breast tumor lesions in the liver following i.v. administration. To localize the metastatic lesions more precisely we did PET-CT scans that enabled us to visualize the heightened glucose metabolism of tumors by the FDG tracer. By combining two molecular imaging techniques that provide metabolic and gene expression information, conferred by FDG-PET and bioluminescence imaging respectively, the specificity of detecting metastases can be greatly enhanced.

Besides strong liver tropism, human adenoviruses exhibit preferential distribution into the lymphatic system (7,8). Its lymphotropic properties can be gleaned from historical evidence that the virus was isolated from adenoids, which collect the majority of lymph drainage of upper respiratory tracts (38). In a recently published report, we were able to successfully target and express PET imaging reporter genes in metastatic prostate cancer tumor cells within draining lymph nodes with a prostate-specific TSTA Ad (8). This current study further verifies the feasibility of exploiting the inherent lymphotropic properties of Ad to query the sentinel lymph node status in a breast tumor model. Employing an approach that parallels clinical lymphoscintigraphy, the AdMUC1-TSTA-fl viral particles were injected peritumorally. We observed that the tumor-selective firefly luciferase signals correlated directly with the Renilla luciferase signals of the marked tumor cells in the sentinel lymph nodes of the breast tumor – bearing cohort. This finding indicates that AdMUC1-TSTA-fl is specific and efficient at detecting sentinel lymph node metastases. Compared with conventional lymphoscintigraphy and the sentinel lymph node biopsy method, this transcriptionally targeted adenoviral-based method of lymphangiography has the advantage of being a noninvasive imaging modality, obviating the need to harvest draining nodes for histologic analyses, thereby eliminating the risk of side effects associated with sentinel lymph node biopsy.

A recent insightful review by Punglia et al. (39) examined the findings of 78 randomized clinical trials in the Early Breast Cancer Trialists' Collaborative Group evaluating the extent of surgery and the use of radiation therapy (40). The definitive message from this thorough review is that improved local control, such as excision to negative margins and the use of additional radiation doses, provided a highly statistically significant improvement in long-term breast cancer survival. The most significant indicators for disease recurrence and poor outcome as reported in this study and others include the number of lymph nodes involved, tumor size and grade, lymphovascular invasion, mitotic index, and Her2 positivity (39,41,42). According to these perspectives, the ability of AdMUC1-TSTA-fl to target lymph node metastasis might

provide an additional tool to achieve better local control. Not only can the tumor-selective Ad be used to express various imaging genes for tumor staging, but the same strategy can be applied to express cytotoxic genes to eradicate lymph node metastasis, offering the potential to reduce systemic tumor spread. The TSTA expression system is particularly amenable to simultaneously express multiple transgenes (43). In particular, we have succeeded in expressing an imaging gene and a therapeutic gene simultaneously using the survivin tumor-specific promoter (31), the MUC1 promoter (44), and the prostate-specific antigen promoter.[7]

We anticipate that a significant challenge to the delivery of gene expression – targeted interventions to the clinic, such as the one described here, would be the immunogenicity of the adenoviral vector (45). To overcome this limitation, we and others have undertaken several approaches to modify the surface properties of the viral capsid in order to reduce its antigenicity and to enhance its stability in circulation (37,46). Other steps taken include transiently dampening the host immune system to prolong vector gene expression (47). Recently, we have adapted a method to synthesize block copolymers with precise control of chain lengths and compositions (48). In turn, these synthetic polymers are used to coat the adenovirus by noncovalent electrostatic interactions. Coated adenoviruses have shown significant improvement in their transductional efficiency in cell culture and in animals.[8] This polymer coating approach in conjunction with further transductional targeting modifications (34) could greatly enhance the specificity and performance of our MUC1-expression–targeted Ad in living subjects. Combination use of this system with various transductional targeting strategies would be a vast improvement upon currently available technologies.

In this study, we illustrated in principle the ability of the Ad-based TSTA gene transfer technology to deliver and express imaging reporter genes specifically in breast tumor metastases in living subjects. Due to the low energy of visible light, optical imaging approaches, such as bioluminescence imaging employed in this study, are unable to detect signals beyond a few centimeters of depth as the photons are scattered or absorbed by tissue. We envision the use of PET-CT to be much more appropriate in the clinics and we recently reported the feasibility of employing a parallel Ad-mediated functional PET imaging method to detect prostate cancer nodal metastasis (8). To continue refining this technology for extension into human studies, we are focused on expanding its targeting capabilities with additional promoters, combining with transductional modifications to increase specificity, and integrating clinically relevant PET-CT approaches. We believe that this system holds great promise and has the potential to significantly impact diagnostic and treatment options for breast cancer patients.

Acknowledgments

We deeply appreciate the technical support provided by Dr. Marxa Figueiredo, Dr. Mai Johnson, Yiwei Lin, and Oh-Joon Kwon.

Grant support: NIH/NCI RO1 CA101904 to L. Wu. S. Huyn is supported by the UCLA Tumor Immunology Training Grant (5-T32-CA009120-29), and a Susan G. Komen Foundation fellowship award.

References

1. Jemal A, Siegel R, Ward E, et al. Cancer statistics, 2008. CA Cancer J Clin 2008;58:71–96. [PubMed: 18287387]

[7]Sato et al, unpublished data.
[8]Koh et al, unpublished data.

2. Gloeckler Ries LA, Reichman ME, Lewis DR, Hankey BF, Edwards BK. Cancer survival and incidence from the Surveillance, Epidemiology, and End Results (SEER) program. Oncologist 2003;8:541–52. [PubMed: 14657533]
3. Achen MG, McColl BK, Stacker SA. Focus on lymphangiogenesis in tumor metastasis. Cancer Cell 2005;7:121–7. [PubMed: 15710325]
4. Samphao S, Eremin JM, El-Sheemy M, Eremin O. Management of the axilla in women with breast cancer: current clinical practice and a new selective targeted approach. Ann Surg Oncol 2008;15:1282–96. [PubMed: 18330650]
5. Crane-Okada R, Wascher RA, Elashoff D, Giuliano AE. Long-term morbidity of sentinel node biopsy versus complete axillary dissection for unilateral breast cancer. Ann Surg Oncol 2008;15:1996–2005. [PubMed: 18415650]
6. Johnson M, Huyn S, Burton J, Sato M, Wu L. Differential biodistribution of adenoviral vector *in vivo* as monitored by bioluminescence imaging and quantitative polymerase chain reaction. Hum GeneTher 2006;17:1262–9.
7. Kishimoto H, Kojima T, Watanabe Y, et al. *In vivo* imaging of lymph node metastasis with telomerase-specific replication-selective adenovirus. Nat Med 2006;12:1213–9. [PubMed: 17013385]
8. Burton JB, Johnson M, Sato M, et al. Adenovirus-mediated gene expression imaging to directly detect sentinel lymph node metastasis of prostate cancer. Nat Med 2008;14:882–8. [PubMed: 18622403]
9. Sato M, Johnson M, Zhang L, et al. Optimization of adenoviral vectors to direct highly amplified prostate-specific expression for imaging and gene therapy. Mol Ther 2003;8:726–37. [PubMed: 14599805]
10. Iyer M, Wu L, Carey M, Wang Y, Smallwood A, Gambhir SS. Two-step transcriptional amplification as a method for imaging reporter gene expression using weak promoters. Proc Natl Acad Sci U S A 2001;98:14595–600. [PubMed: 11734653]
11. Johnson M, Sato M, Burton JB, Gambhir SS, Carey M, Wu L. Micro-PET/CT monitoring of herpes thymidine kinase suicide gene therapy in a prostate cancer xenograft: the advantage of a cell-specific transcriptional targeting approach. Mol Imaging 2005;4:463–72. [PubMed: 16285908]
12. Chen L, Chen D, Manome Y, Dong Y, Fine HA, Kufe DW. Breast cancer selective gene expression and therapy mediated by recombinant adenoviruses containing the DF3/MUC1 promoter. J Clin Invest 1995;96:2775–82. [PubMed: 8675647]
13. Abe M, Kufe D. Characterization of cis-acting elements regulating transcription of the human DF3 breast carcinoma-associated antigen (MUC1) gene. Proc Natl Acad Sci USA 1993;90:282–6. [PubMed: 8419933]
14. Kovarik A, Peat N, Wilson D, Gendler SJ, Taylor-Papadimitriou J. Analysis of the tissue-specific promoter of the MUC1 gene. J Biol Chem 1993;268:9917–26. [PubMed: 8387509]
15. Walsh MD, Luckie SM, Cummings MC, Antalis TM, McGuckin MA. Heterogeneity of MUC1 expression by human breast carcinoma cell lines *in vivo* and *in vitro*. Breast Cancer Res Treat 1999;58:255–66. [PubMed: 10718487]
16. Hilkens J, Vos HL, Wesseling J, et al. Is episialin/MUC1 involved in breast cancer progression? Cancer Lett 1995;90:27–33. [PubMed: 7720039]
17. Zhang K, Sikut R, Hansson GC. A MUC1 mucin secreted from a colon carcinoma cell line inhibits target cell lysis by natural killer cells. Cell Immunol 1997;176:158–65. [PubMed: 9073389]
18. Schwartz, M. Cancer markers. In: DeVita, VT.; Hellman, S.; Rosenberg, SA., editors. Cancer: principles and practice of oncology. Lippincott; 1993. p. 531-42.
19. Finn OJ, Jerome KR, Henderson RA, et al. MUC-1 epithelial tumor mucin-based immunity and cancer vaccines. Immunol Rev 1995;145:61–89. [PubMed: 7590831]
20. Block A, Milasinovic D, Mueller J, Schaefer P, Schaefer H, Greten H. Amplified Muc1-specific gene expression in colon cancer cells utilizing a binary system in adenoviral vectors. Anticancer Res 2002;22:3285–92. [PubMed: 12530077]
21. He TC, Zhou S, da Costa LT, Yu J, Kinzler KW, Vogelstein B. A simplified system for generating recombinant adenoviruses. Proc Natl Acad Sci U S A 1998;95:2509–14. [PubMed: 9482916]
22. Zhang L, Adams JY, Billick E, et al. Molecular engineering of a two-step transcription amplification (TSTA) system for transgene delivery in prostate cancer. Mol Ther 2002;5:223–32. [PubMed: 11863411]

23. Brakenhielm E, Burton JB, Johnson M, et al. Modulating metastasis by a lymphangiogenic switch in prostate cancer. Int J Cancer 2007;121:2153–61. [PubMed: 17583576]
24. Chow PL, Stout DB, Komisopoulou E, Chatziioannou AF. A method of image registration for small animal, multi-modality imaging. Phys Med Biol 2006;51:379–90. [PubMed: 16394345]
25. Kurebayashi J, Kurosumi M, Sonoo H. A new human breast cancer cell line, KPL-1 secretes tumour-associated antigens and grows rapidly in female athymic nude mice. Br J Cancer 1995;71:845–53. [PubMed: 7710953]
26. Adams JY, Johnson M, Sato M, et al. Visualization of advanced human prostate cancer lesions in living mice by a targeted gene transfer vector and optical imaging. Nat Med 2002;8:891–7. [PubMed: 12134144]
27. Skobe M, Hawighorst T, Jackson DG, et al. Induction of tumor lymphangiogenesis by VEGF-C promotes breast cancer metastasis. Nat Med 2001;7:192–8. [PubMed: 11175850]
28. Lu X, Kang Y. Organotropism of breast cancer metastasis. J Mammary Gland Biol Neoplasia 2007;12:153–62. [PubMed: 17566854]
29. Wang Y, Iyer M, Annala A, Wu L, Carey M, Gambhir SS. Noninvasive indirect imaging of vascular endothelial growth factor gene expression using bioluminescence imaging in living transgenic mice. Physiol Genomics 2006;24:173–80. [PubMed: 16410544]
30. Xie X, Xia W, Li Z, et al. Targeted expression of BikDD eradicates pancreatic tumors in noninvasive imaging models. Cancer Cell 2007;12:52–65. [PubMed: 17613436]
31. Ray S, Paulmurugan R, Patel MR, et al. Noninvasive imaging of therapeutic gene expression using a bidirectional transcriptional amplification strategy. Mol Ther 2008;16:1848–56. Epub 2008 Sep 2. [PubMed: 18766175]
32. Alemany R, Curiel DT. CAR-binding ablation does not change biodistribution and toxicity of adenoviral vectors. Gene Ther 2001;8:1347–53. [PubMed: 11571572]
33. Shayakhmetov DM, Li ZY, Ni S, Lieber A. Analysis of adenovirus sequestration in the liver, transduction of hepatic cells, and innate toxicity after injection of fiber-modified vectors. J Virol 2004;78:5368–81. [PubMed: 15113916]
34. Li HJ, Everts M, Pereboeva L, et al. Adenovirus tumor targeting and hepatic untargeting by a coxsackie/adenovirus receptor ectodomain anti-carcinoembryonic antigen bispecific adapter. Cancer Res 2007;67:5354–61. [PubMed: 17545616]
35. Waddington SN, McVey JH, Bhella D, et al. Adenovirus serotype 5 hexon mediates liver gene transfer. Cell 2008;132:397–409. [PubMed: 18267072]
36. Kalyuzhniy O, Di Paolo NC, Silvestry M, et al. Adenovirus serotype 5 hexon is critical for virus infection of hepatocytes *in vivo*. Proc Natl Acad Sci U S A 2008;105:5483–8. [PubMed: 18391209]
37. Glasgow JN, Bauerschmitz GJ, Curiel DT, Hemminki A. Transductional and transcriptional targeting of adenovirus for clinical applications. Curr Gene Ther 2004;4:1–14. [PubMed: 15032610]
38. van der Veen J, Lambriex M. Relationship of adenovirus to lymphocytes in naturally infected human tonsils and adenoids. Infect Immun 1973;7:604–9. [PubMed: 4796933]
39. Punglia RS, Morrow M, Winer EP, Harris JR. Local therapy and survival in breast cancer. N Engl J Med 2007;356:2399–405. [PubMed: 17554121]
40. Clarke M, Collins R, Darby S, et al. Effects of radiotherapy and of differences in the extent of surgery for early breast cancer on local recurrence and 15-year survival: an overview of the randomised trials. Lancet 2005;366:2087–106. [PubMed: 16360786]
41. Soerjomataram I, Louwman MW, Ribot JG, Roukema JA, Coebergh JW. An overview of prognostic factors for long-term survivors of breast cancer. Breast Cancer Res Treat 2008;107:309–30. [PubMed: 17377838]
42. Schoppmann SF, Bayer G, Aumayr K, et al. Prognostic value of lymphangiogenesis and lymphovascular invasion in invasive breast cancer. Ann Surg 2004;240:306–12. [PubMed: 15273556]
43. Ray S, Paulmurugan R, Hildebrandt I, et al. Novel bidirectional vector strategy for amplification of therapeutic and reporter gene expression. Hum Gene Ther 2004;15:681–90. [PubMed: 15242528]
44. Huyn, S.; Sato, M.; Johnson, M.; Burton, JB.; Wu, L. Development of a highly efficient targeted gene therapy vector for the treatment and diagnosis of metastatic breast cancer. American Society of Gene Therapy; Seattle, Washington: 2007.

45. Bangari DS, Mittal SK. Current strategies and future directions for eluding adenoviral vector immunity. Curr Gene Ther 2006;6:215–26. [PubMed: 16611043]

46. Fisher KD, Stallwood Y, Green NK, Ulbrich K, Mautner V, Seymour LW. Polymer-coated adenovirus permits efficient retargeting and evades neutralising antibodies. Gene Ther 2001;8:341–8. [PubMed: 11313809]

47. Lamfers ML, Fulci G, Gianni D, et al. Cyclophosphamide increases transgene expression mediated by an oncolytic adenovirus in glioma-bearing mice monitored by bioluminescence imaging. Mol Ther 2006;14:779–88. [PubMed: 16996314]

48. Demming T. Living polymerization of á-amino acid-N-carboxyanhydrides. J Polymer Sci 2000;38:3011–8.

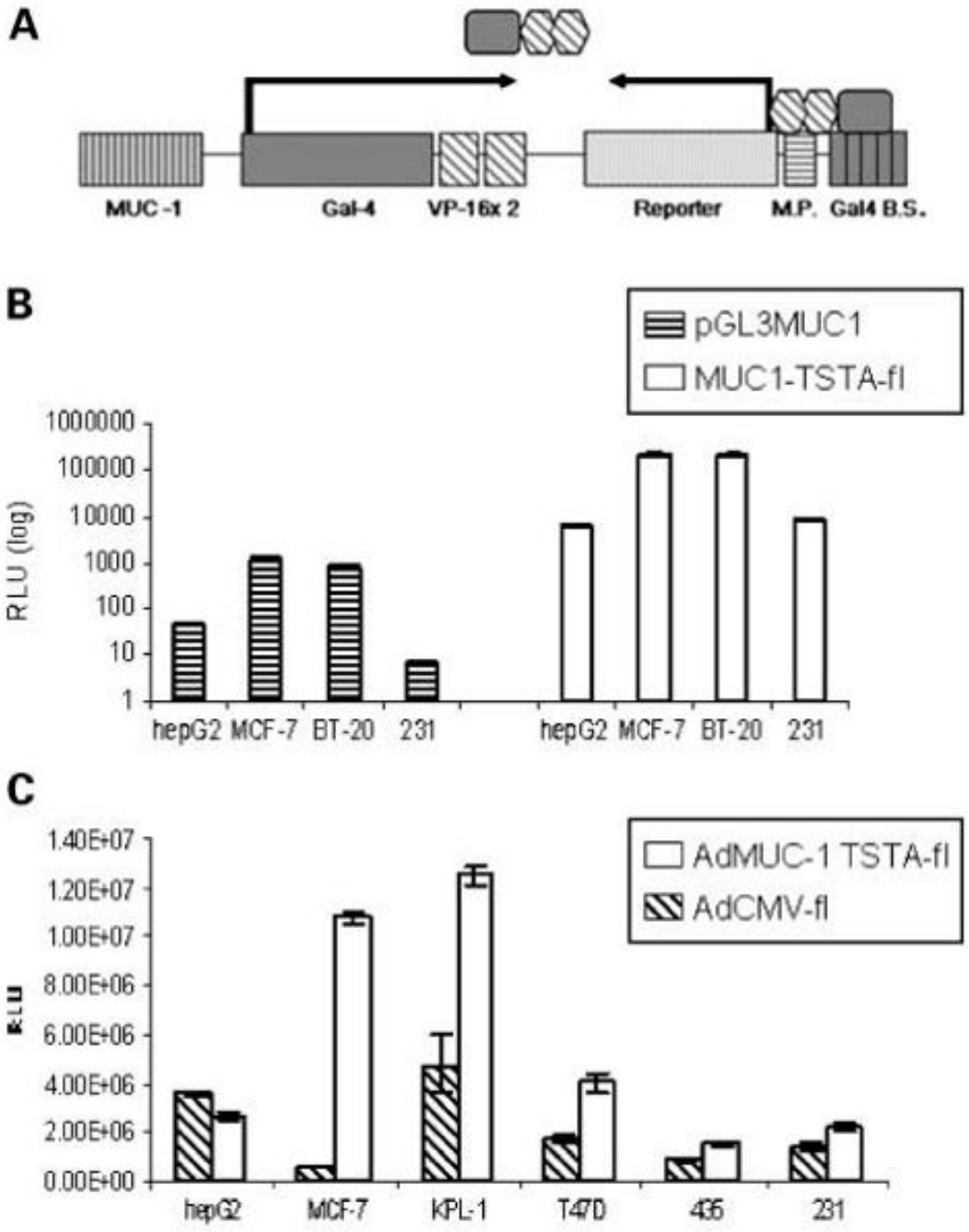

Fig. 1.

Schematic of the MUC1-TSTA system and *in vitro* analysis. *A*, schematic showing the MUC-1 TSTA amplification scheme in the all-in-one tail-to-tail configuration. In this construct, the MUC-1 promoter (-780 to +50) drives the expression of a Gal-4 VP-16 fusion protein, which acts as a potent synthetic transcriptional activator. This fusion protein then binds to the Gal4 recognition sites upstream of a minimal promoter that activates the expression of a reporter gene or therapeutic gene. *B*, 0.5×10^5 breast (MCF-7, BT-20, MDA-MB-231) and nonbreast (hepG2) cells were transfected with either the pGL3MUC1 direct expression vector (*striped*) or the pMUC1 TSTA reporter system pMUC1-TSTA-fl (*white*). Normalized firefly luciferase activities, analyzed at 48 h after transfection, were recorded as RLU/s; data are expressed in

log scale. *Columns*, averages of three transfections; *bars*, SE. *C*, breast (MCF-7, KPL-1, T47D, MDA-MB-435, MDA-MB-231) and nonbreast (hepG2) cell lines were infected by AdMUC1-TSTA-fl (*white*) and AdCMV-fl (*striped*) at an MOI = 5. Firefly luciferase activity in the infected cells measured as RLU/s were evaluated at 48 h after infection. *Columns*, averages of three infections; *bars* SE.

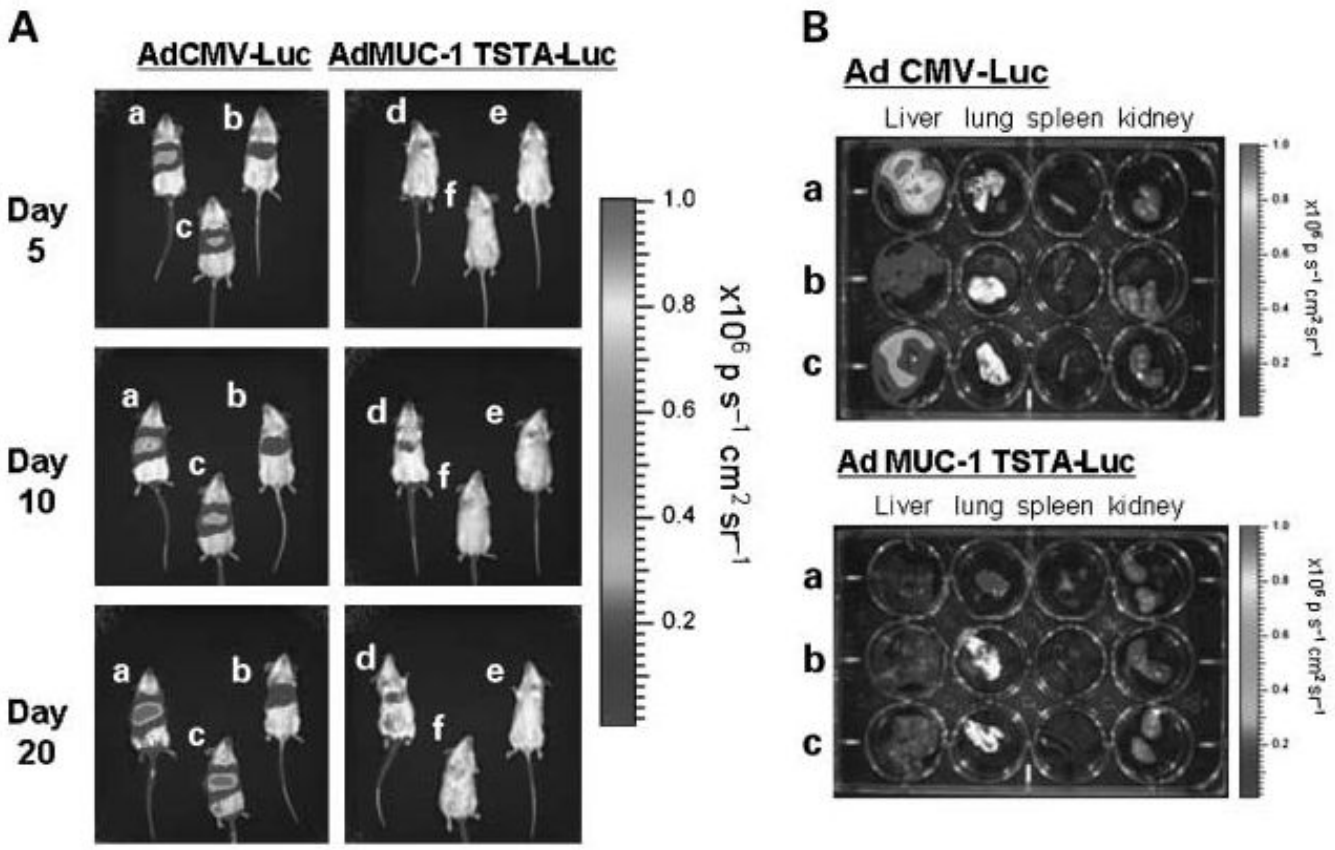

Fig. 2.

In vivo off-target expression analysis. Non – tumor-bearing female SCID mice were given i.v. injections of either AdCMV-fl ($n = 6$) or AdMUC1-TSTA-fl ($n = 6$) virus at 1×10^7 pfu. *A*, mice were optically imaged for firefly luciferase expression at 5, 10, and 20 d postinjection. Three representative animals from each cohort were shown. *B*, at day 20, the mice were sacrificed, and their organs (liver, lung, spleen, kidney) were harvested and imaged for firefly luciferase expression *ex vivo* (photons/s^{-1} cm^2 sr^{-1}).

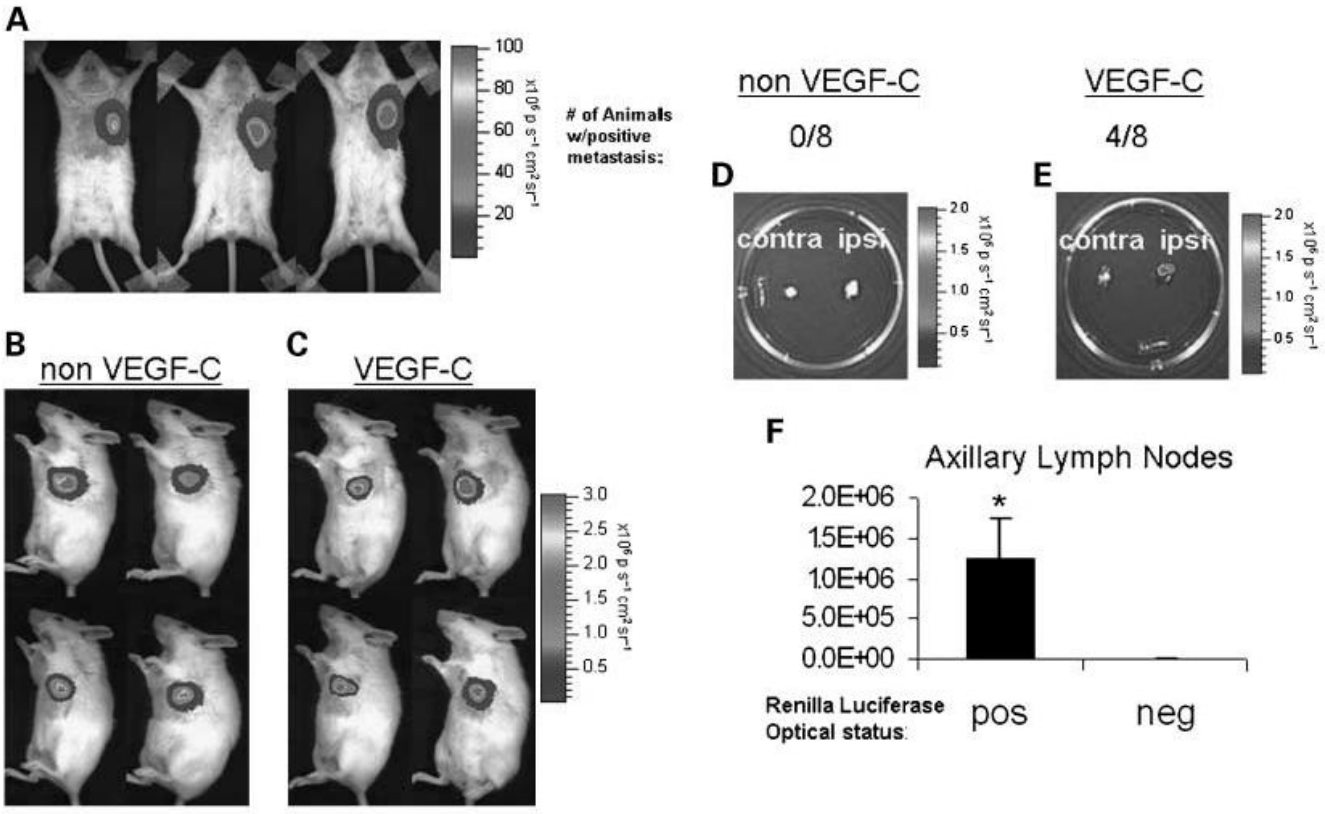

Fig. 3.

VEGF-C overexpression induces KPL-1 lymph node metastasis. *A*, KPL-1 tumors grown to ~ 1cm in female SCID beige mice ($n = 6$) were injected intratumorally with 1×10^8 pfu of AdMUC1-TSTA-fl. Three days postinjection, the animals were assessed for firefly luciferase expression by MS 100 and images from three representative animals are shown. KPL-1 tumor cells were implanted into the mammary fat pads of female SCID beige mice following double marking with lenti-CMV-rl and either a (*B*) lenti-CMV-IRES-EGFP control virus ($n = 8$) or a (*C*) lenti-CMV-VEGF-C-IRES-EGFP virus ($n = 8$). Cells were implanted into the mammary fat pads of SCID beige mice. After the tumors were grown for 4 wk, reaching ~ 1 cm diameter, the animals were imaged for renilla luciferase expression; four representative animals from each group are shown (*B, C*). At the terminal time point both axillary lymph nodes, ipsilateral and contralateral to the primary tumor, were extracted and imaged *ex vivo* for tumor cell infiltration by renilla luciferase activity; the axillary lymph nodes from one representative animal from each group are displayed (*D, E*). In the non – VEGF-C group 0 of 8 animals developed lymph node metastasis, whereas 4 of 8 animals in theVEGF-C – expressing group developed lymph node metastasis. *F*, the regions of interest for optically positive lymph nodes were compared with optically negative nodes. *Columns*, averages of regions of interest, *bars*, SE, *, $P < 0.05$.

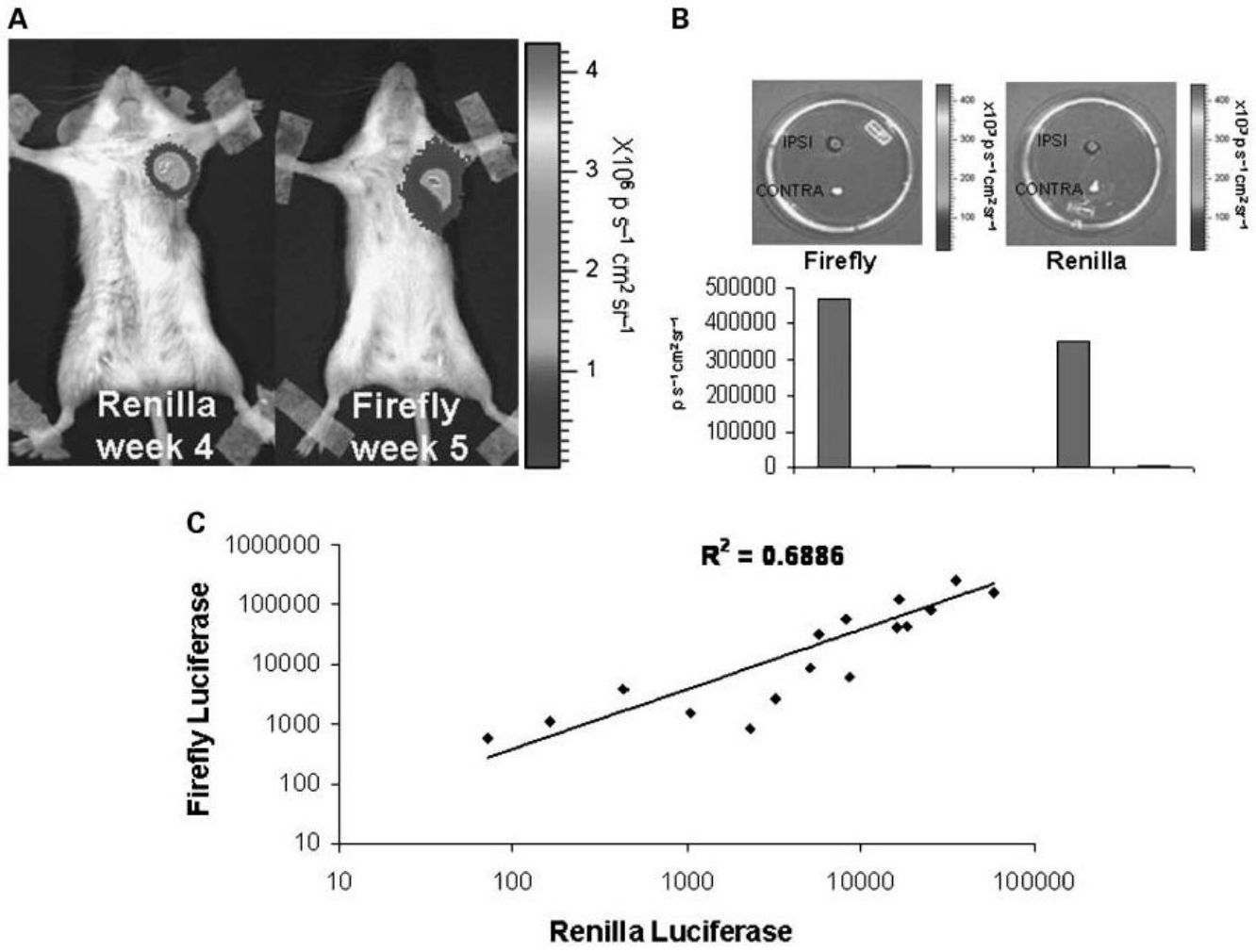

Fig. 4.

AdMUC1-TSTA-fl targeting of axillary lymph node metastasis. *A, in vivo* optical imaging of both renilla and firefly luciferase expression from a peritumorally injected AdMUC1 -TSTA-fI, lenti-CMV-RL/lenti-CMV-VEGF-C double marked KPL-1 tumor-bearing animal. *B*, both the ipsilateral and contralateral axillary lymph nodes from the representative animal were extracted and sequentially imaged *ex vivo* for both firefly and renilla luciferase expression. Bioluminesence intensity for each lymph node was calculated using living image software and plotted below its corresponding image. Four of eight animals showed positivity for both renilla luciferase expression and firefly luciferase expression. *C*, axillary lymph nodes from the entire cohort ($n = 8$) were digested using passive lysis buffer; lysates were analyzed by dual luciferase assay. Firefly luciferase activity was plotted against renilla luciferase activity resulting in $R^2 = 0.686$ ($P < 0.05$).

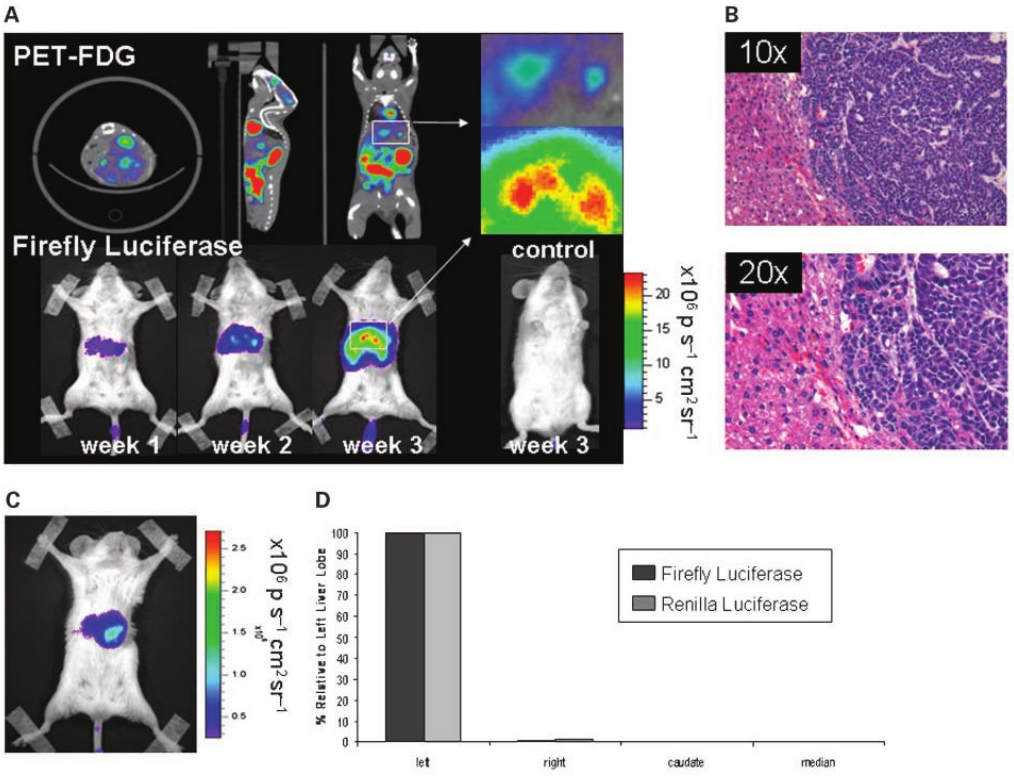

Fig. 5.

AdMUC1-TSTA-fl targeting of liver metastasis. *A*, PET imaging using 2-[^{18}F] -fluoro-2-deoxy-D-glucose (^{18}FDG) at 2 wk post – KPL-1 tumor implantation. Transverse, sagittal, and coronal images are displayed. The white box highlights tumor signal. Following PET imaging, hepatic tumor-bearing mice and non – tumor-bearing control animals were given 1×10^8 pfu of Ad MUC1-TSTA-fI i.v. Optical imaging for firefly luciferase was carried out at 1, 2, and 3 wk postinjection (*A*). *B*, The left lobes of a targeted hepatic tumor-bearing animal was extracted, fixed, sectioned, and stained with H&E. *C*, a separate animal bearing a KPL-1 hepatic tumor was systemically targeted using AdMUC1-TSTA-fl and imaged. *D*, following targeting, the liver was extracted and the left, right, median, and caudate lobes were mechanically digested, and lysed in passive lysis buffer. Supernatant was assayed for both firefly and renilla luciferase expression. Ad-mediated firefly luciferase activity in each lobe (*black bar*) relative to maximal signal in the left lobe (100%) is plotted along side with tumor cell-directed relative renilla luciferase activity (*grey bar*).